Lepton polarization and CP-violating effects in $\overline{B} \to \overline{K}_0^*(1430)\ell^+\ell^-$ Decay in Standard and Two Higgs Doublet Model

F. Falahati[a*], S. M. Zebarjad and S. Naeimipour

[a]*Physics Department and Biruni Observatory, College of Sciences, Shiraz University, Shiraz 71454, Iran*

In this paper we analyze the dilepton mass square q^2 dependency of single lepton polarization asymmetries and CP violation for $\overline{B} \to \overline{K}_0^*(1430)\ell^+\ell^-, \ell = \mu, \tau$) in the 2HDM context. Also, we study the averages of these asymmetries in the domain $4m_\ell^2 < q^2 < (m_B - m_{K_0^*})^2$. Our study manifests that the investigation of the above-mentioned asymmetries for $\overline{B} \to \overline{K}_0^*(1430)\ell^+\ell^-$ processes could provide useful information for probing new Higgs bosons in the future B-physics experiments.

Packs numbers: 12.60.-i, 13.30.-a, 14.20.Mr

arXiv:1510.02936v1 [hep-ph] 10 Oct 2015

I. INTRODUCTION

Now that last missing ingredient of the Standard Model (SM) (SM Higgs particle) has been experimentally discovered at the LHC by the ATLAS [1] and CMS [2, 3] collaborations, with a mass $m_H \simeq 125$ GeV, the possibility of discovery of an enlarged scalar sector becomes very plausible. On the other hand, between the spectrum of extensions of the SM, there are predictions that anticipate more than one scalar Higgs doublet; for instance, the case of the Minimal- Supersymmetric-Standard-Model (MSSM)). Based on this we can consider a prototype of extensions of the SM which are including a larger scalar sector, called generically the Two- Higgs-Doublet-Model (2HDM). There are different types of such 2HDM models. In the model called type I, one Higgs doublet generates masses for the up and down quarks, simultaneously. In the model type II, one Higgs doublet gives masses to the up-type quarks and the other one to the down-type quarks. These two models include a discrete symmetry to prevent flavour changing neutral currents (FCNC) at tree level. However, the addition of these discrete symmetries is not required and in this case both doublets are contributing to provide the masses to up-type and down-type quarks. In the literature, such a model is known as the 2HDM type III . It has been used to search for physics beyond the SM and specifically for FCNC at tree level. In general, both doublets can acquire a vacuum expectation value (VEV), but one of them can be absorbed redefining the Higgs boson fields properly. Nevertheless, other studies on 2HDM-III using different basis have been done and there is a case where both doublets get VEVs that allows to study the models type I and II in a specific limit[4, 32].

In the 2HDM models, the two complex Higgs doublets include eigth scalar states. Spontanoues Symmetry breaking procedure generates five Higgs fields: two neutral CP-even scalars h^0 and H^0, a neutral CP-odd scalar A^0, and two charged scalars H. While the neutral Higgs bosons may be difficult to distinguish from the one of the SM, the charged Higgs bosons would have a distinctive signal for physics beyond the SM. Therefore the direct or indirect effect of a charged Higgs boson would play an important role in the discovery of an extended Higgs model. The limitations which come from the experimental results of $B - \bar{B}$ mixing, $\Gamma(b \to s\gamma)$, $\Gamma(b \to c\tau\bar{\nu}_\tau)$, ρ_0, R_b and the electric dipole moments (EDMS) of the electron and neutron[30, 32, 37, 38] could constrain the range of variation of masses of Higgs bosons and that of the other related parameters such as vertex parameters, λ_{tt} and λ_{bb}.

FCNC and CP-violating are indeed the most sensitive probes of NP contributions to penguin operators. Rare decays, induced by FCNC of $b \to s\ell^+\ell^-(\ell = e, \mu, \tau)$ transitions are at the forefront of our quest to understand flavor and the origins of CP violation asymmetry (CPV), offering one of the best probes for NP beyond the SM, in particular to explore 2HDM.

* falahati@shirazu.ac.ir

Although the branching ratios of FCNC decays are small in the SM, interesting results are yielded in developing experiments. The inclusive $b \to X_s \ell^+ \ell^-$ decay is observed in BaBaR [12] and Belle collaborations. These collaborations also measured exclusive modes $B \to K \ell^+ \ell^-$ [13–15] and $B \to K^* \ell^+ \ell^-$ [16]. These experimental results show high agreement with theoretical predictions [17–19].

There exists another group of rare decays induced by $b \to s$ transition, such as $B \to K_2^*(1430)\ell^+\ell^-$ and $B \to K_0^*(1430)\ell^+\ell^-$ in which B meson decays into a tensor or scalar meson, respectively. These decays are deeply investigated in SM in [20, 21] and the related transition form factors are formulated within the framework of light front quark model [21–23] and QCD sum rules method [24, 25], respectively.

In this paper, we will investigate the exclusive decay $\overline{B} \to \overline{K}_0^*(1430)\ell^+\ell^-(\ell = \mu, \tau)$, where $\overline{K}_0^*(1430)$ is a scalar meson, both in the SM and 2HDM. We evaluate the single lepton polarization asymmetries and CP violating effects with special emphasis on the model III of 2HDM.

The paper is organized as follows. In Section II, we describe the content of the general 2HDM and write down the Yukawa Lagrangian for model III. In Section III, the effective Hamiltonian and matrix elements of $\overline{B} \to \overline{K}_0^*(1430)\ell^+\ell^-$ transition in SM and 2HDM are presented. Then the general expressions for single lepton polarization asymmetries and CP violation have been extracted out. Section IV is devoted to discussion and our conclusions. In the final section a brief summery of our results is presented.

II. THE GENERAL TWO-HIGGS-DOUBLET MODEL

In a general two-Higgs-doublet model, both the doublets can couple to the up-type and down-type quarks. Without missing any thing, we use a basis such that the first doublet produces the masses of all the gauge-bosons and fermions[32]:

$$\langle \phi_1 \rangle = \begin{pmatrix} 0 \\ \frac{v}{\sqrt{2}} \end{pmatrix}, \qquad \langle \phi_2 \rangle = 0 \tag{1}$$

where v is due to the W mass by $M_W = \frac{g}{2}v$. Based on this, the first doublet ϕ_1 is the same as the SM doublet, whereas all the new Higgs fields originate from the second doublet ϕ_2. They are written as

$$\phi_1 = \frac{1}{\sqrt{2}} \begin{pmatrix} \sqrt{2}G^+ \\ v + \chi_1^0 + iG^0 \end{pmatrix}, \qquad \phi_2 = \frac{1}{\sqrt{2}} \begin{pmatrix} \sqrt{2}H^+ \\ \chi_2^0 + iA^0 \end{pmatrix}, \tag{2}$$

where G^0 and $G^\pm$ are the Goldstone bosons that would be absorbed in the Higgs mechanism to provide the longitudinal components of the weak gauge bosons. The $H^\pm$ are the physical charged-Higgs bosons and A^0 is the physical CP-odd neutral Higgs boson. The χ_1^0 and χ_2^0 are not physical mass eigenstates but are written as linear combinations of the CP-even neutral Higgs bosons:

$$\chi_1^0 = H^0 \cos\alpha - h^0 \sin\alpha \tag{3}$$

$$\chi_2^0 = H^0 \sin\alpha + h^0 \cos\alpha\,, \tag{4}$$

where α is the mixing angle. Using this basis, the couplings of $\chi_2^0 ZZ$ and $\chi_2^0 W^+W^-$ are disappeared. We can present[34] the Yukawa Lagrangian for model III as

$$-\mathscr{L}_Y = \eta_{ij}^U \overline{Q_{iL}} \tilde{\phi}_1 U_{jR} + \eta_{ij}^D \overline{Q_{iL}} \phi_1 D_{jR} + \xi_{ij}^U \overline{Q_{iL}} \tilde{\phi}_2 U_{jR} + \xi_{ij}^D \overline{Q_{iL}} \phi_2 D_{jR} \quad + \text{h.c.}\,, \tag{5}$$

where i, j are generation indices, $\tilde{\phi}_{1,2} = i\sigma_2 \phi_{1,2}$, $\eta_{ij}^{U,D}$ and $\xi_{ij}^{U,D}$ are, in general, nondiagonal coupling matrices, and Q_{iL} is the left-handed fermion doublet and U_{jR} and D_{jR} are the right-handed singlets. Note that these Q_{iL}, U_{jR}, and D_{jR} are weak eigenstates, which can be expanded by mass eigenstates. As we have mentioned above, ϕ_1 provides all the fermion masses and, therefore, $\frac{v}{\sqrt{2}}\eta^{U,D}$ will become the up- and down-type quark-mass matrices after a bi-unitary transformation. Applying the transformation the Yukawa Lagrangian becomes

$$\begin{aligned} \mathscr{L}_Y &= -\overline{U}M_U U - \overline{D}M_D D - \frac{g}{2M_W}(H^0\cos\alpha - h^0\sin\alpha)\left(\overline{U}M_U U + \overline{D}M_D D\right) \\ &+ \frac{ig}{2M_W} G^0 \left(\overline{U}M_U \gamma^5 U - \overline{D}M_D \gamma^5 D\right) \end{aligned}$$

$$
\begin{aligned}
&+ \frac{g}{\sqrt{2}M_W} G^- \overline{D} V_{\rm CKM}^\dagger \left[M_U \tfrac{1}{2}(1+\gamma^5) - M_D \tfrac{1}{2}(1-\gamma^5) \right] U \\
&- \frac{g}{\sqrt{2}M_W} G^+ \overline{U} V_{\rm CKM} \left[M_D \tfrac{1}{2}(1+\gamma^5) - M_U \tfrac{1}{2}(1-\gamma^5) \right] D \\
&- \frac{H^0 \sin\alpha + h^0 \cos\alpha}{\sqrt{2}} \left[\overline{U} \left(\hat{\xi}^U \tfrac{1}{2}(1+\gamma^5) + \hat{\xi}^{U\dagger} \tfrac{1}{2}(1-\gamma^5) \right) U \right. \\
&\quad \left. + \overline{D} \left(\hat{\xi}^D \tfrac{1}{2}(1+\gamma^5) + \hat{\xi}^{D\dagger} \tfrac{1}{2}(1-\gamma^5) \right) D \right] \\
&+ \frac{iA^0}{\sqrt{2}} \left[\overline{U} \left(\hat{\xi}^U \tfrac{1}{2}(1+\gamma^5) - \hat{\xi}^{U\dagger} \tfrac{1}{2}(1-\gamma^5) \right) U - \overline{D} \left(\hat{\xi}^D \tfrac{1}{2}(1+\gamma^5) - \hat{\xi}^{D\dagger} \tfrac{1}{2}(1-\gamma^5) \right) D \right] \\
&- H^+ \overline{U} \left[V_{\rm CKM} \hat{\xi}^D \tfrac{1}{2}(1+\gamma^5) - \hat{\xi}^{U\dagger} V_{\rm CKM} \tfrac{1}{2}(1-\gamma^5) \right] D \\
&- H^- \overline{D} \left[\hat{\xi}^{D\dagger} V_{\rm CKM}^\dagger \tfrac{1}{2}(1-\gamma^5) - V_{\rm CKM}^\dagger \hat{\xi}^U \tfrac{1}{2}(1+\gamma^5) \right] U \ , \qquad (6)
\end{aligned}
$$

where U is a symbol for the mass eigenstates of u,c,t quarks and D is a symbol for the mass eigenstates of d,s,b quarks. The diagonal mass matrices are defined by $M_{U,D} = \text{diag}(m_{u,d}, m_{c,s}, m_{t,b}) = \frac{v}{\sqrt{2}} (\mathscr{L}_{U,D})^\dagger \eta^{U,D} (\mathscr{R}_{U,D})$, $\hat{\xi}^{U,D} = (\mathscr{L}_{U,D})^\dagger \xi^{U,D} (\mathscr{R}_{U,D})$. The Cabibbo-Kobayashi-Maskawa matrix [5] is given by $V_{\rm CKM} = (\mathscr{L}_U)^\dagger (\mathscr{L}_D)$.

The matrices $\hat{\xi}^{U,D}$ contain the FCNC couplings. These matrices would be given as [6]:

$$
\hat{\xi}^{U,D}_{ij} = \lambda_{ij} \frac{g\sqrt{m_i m_j}}{\sqrt{2}M_W} \qquad (7)
$$

by which the quark-mass hierarchy is ensured while the FCNC for the first two generations are suppressed by the small quark masses, is allowed for the third generation.

III. ANALYTIC FORMULAS

A. The Effective Hamiltonian for $\overline{B} \to \overline{K}_0^*(1430)\ell^+\ell^-$ transition in SM and 2HDM

The exclusive decay $\overline{B} \to \overline{K}_0^*(1430)\ell^+\ell^-$ is described at quark level by $b \to s\ell^+\ell^-$ transition. Taking into account the additional Higgs boson exchange diagrams, the effective Hamiltonian is calculated in 2HDM as:

$$
\mathscr{H}_{eff}(b \to s\ell^+\ell^-) = -\frac{4G_F}{\sqrt{2}} V_{tb} V_{ts}^* \left\{ \sum_{i=1}^{10} C_i(\mu) O_i(\mu) + \sum_{i=1}^{10} C_{Q_i}(\mu) Q_i(\mu) \right\} \ , \qquad (8)
$$

where the first set of operators in the brackets are due to the SM effective Hamiltonian. Also note that the contributions of charged Higgs diagrams are taken into account in the aforementioned set of operators by modifying the corresponding Wilson coefficients. The second part which includes new operators is extracted from contribution of the massive neutral Higgs bosons to this decay. All operators as well as the related Wilson coefficients are given in [33–35]. Now, using the above effective Hamiltonian, the one-loop matrix elements of $b \to s\ell^+\ell^-$ can be given as:

$$
\begin{aligned}
\mathscr{M} &= < s\ell^+\ell^- | \mathscr{H}_{\rm eff} | b > \\
&= -\frac{G_F \alpha}{2\sqrt{2}\pi} V_{tb} V_{ts}^* \left\{ \tilde{C}_9^{\rm eff} \bar{s}\gamma_\mu (1-\gamma_5) b \, \bar{\ell}\gamma^\mu \ell + \tilde{C}_{10} \bar{s}\gamma_\mu (1-\gamma_5) b \, \bar{\ell}\gamma^\mu \gamma_5 \ell \right. \\
&- 2C_7^{\rm eff} \frac{m_b}{q^2} \bar{s} i\sigma_{\mu\nu} q^\nu (1+\gamma_5) b \, \bar{\ell}\gamma^\mu \ell - 2C_7^{\rm eff} \frac{m_s}{q^2} \bar{s} i\sigma_{\mu\nu} q^\nu (1-\gamma_5) b \, \bar{\ell}\gamma^\mu \ell \\
&+ \left. C_{Q_1} \bar{s}(1+\gamma_5) b \, \bar{\ell}\ell + C_{Q_2} \bar{s}(1+\gamma_5) b \, \bar{\ell}\gamma_5 \ell \right\} . \qquad (9)
\end{aligned}
$$

The Wilson coefficients $C_7^{\rm eff}$, $\tilde{C}_9^{\rm eff}$, $\tilde{C}_{10}$ are obtained from their SM values by adding the contributions due to the charged Higgs bosons exchange diagrams. Note that this addition is performed at high m_W scale, and then using the renormalization group equations, the coefficients are calculated at lower m_b scale. Coefficients C_{Q_1} and C_{Q_2} describe the neutral Higgs boson exchange diagrams' contributions. The operators $O_i (i = 1, \cdots, 10)$ do not mix with Q_1 and Q_2 and there is no mixing between Q_1 and Q_2. For this reason the evolutions of the coefficients C_{Q_1} and C_{Q_2} are controlled by the anomalous dimensions of Q_1 and Q_2 respectively[35]:

$$C_{Q_i}(m_b) = \eta^{-\gamma_Q/\beta_0} C_{Q_i}(m_W)\ , \quad i = 1,\ 2,$$

where $\gamma_Q = -4$ is the anomalous dimension of the operator $\bar{s}_L b_R$.

The coefficients $C_i(m_W)$ ($i = 7, 9$ and 10) and $C_{Q_1}(m_W)$ and $C_{Q_2}(m_W)$ are given by:

$$\begin{aligned} C_7(m_W) &= x\frac{(7-5x-8x^2)}{24(x-1)^3} + \frac{x^2(3x-2)}{4(x-1)^4}\ln x \\ &+ |\lambda_{tt}|^2\left(\frac{y(7-5y-8y^2)}{72(y-1)^3} + \frac{y^2(3y-2)}{12(y-1)^4}\ln y\right) \\ &+ \lambda_{tt}\lambda_{bb}\left(\frac{y(3-5y)}{12(y-1)^2} + \frac{y(3y-2)}{6(y-1)^3}\ln y\right), \end{aligned} \tag{10}$$

$$\begin{aligned} C_9(m_W) &= -\frac{1}{sin^2\theta_W}B(m_W) + \frac{1-4sin^2\theta_W}{sin^2\theta_W}C(m_W) \\ &+ \frac{x^2(25-19x)}{36(x-1)^3} + \frac{-3x^4+30x^3-54x^2+32x-8}{18(x-1)^4}\ln x + \frac{4}{9} \\ &+ |\lambda_{tt}|^2\left[\frac{1-4sin^2\theta_W}{sin^2\theta_W}\frac{xy}{8}\left(\frac{1}{y-1} - \frac{1}{(y-1)^2}\ln y\right)\right. \\ &- \left. y\left(\frac{47y^2-79y+38}{108(y-1)^3} - \frac{3y^3-6y^3+4}{18(y-1)^4}\ln y\right)\right], \end{aligned} \tag{11}$$

$$\begin{aligned} C_{10}(m_W) &= \frac{1}{sin^2\theta_W}\Big(B(m_W) - C(m_W)\Big) \\ &+ |\lambda_{tt}|^2\frac{1}{sin^2\theta_W}\frac{xy}{8}\left(-\frac{1}{y-1} + \frac{1}{(y-1)^2}\ln y\right), \end{aligned} \tag{12}$$

$$\begin{aligned} C_{Q_1}(m_W) &= \frac{m_b m_\ell}{m_{h^0}^2}\frac{1}{|\lambda_{tt}|^2}\frac{1}{sin^2\theta_W}\frac{x}{4}\left\{\Big(sin^2\alpha + h\,cos^2\alpha\Big)\,f_1(x,y) + \right. \\ &+ \left[\frac{m_{h^0}^2}{m_W^2} + \Big(sin^2\alpha + h\,cos^2\alpha\Big)(1-z)\right] f_2(x,y) + \\ &+ \left.\frac{sin^2 2\alpha}{2m_{H^\pm}^2}\left[m_{h^0}^2 - \frac{(m_{h^0}^2 + m_{H^0}^2)^2}{2m_{H^0}^2}\right] f_3(y)\right\}, \end{aligned} \tag{13}$$

$$C_{Q_2}(m_W) = -\frac{m_b m_\ell}{m_{A^0}^2}\frac{1}{|\lambda_{tt}|^2}\left\{f_1(x,y) + \left[1 + \frac{m_{H^\pm}^2 - m_{A^0}^2}{m_W^2}\right] f_2(x,y)\right\}, \tag{14}$$

where

$$x = \frac{m_t^2}{m_W^2}\ , \quad y = \frac{m_t^2}{m_{H^\pm}^2}\ , \quad z = \frac{x}{y}\ , \quad h = \frac{m_{h^0}^2}{m_{H^0}^2}\ ,$$

$$
\begin{aligned}
B(x) &= -\frac{x}{4(x-1)}+\frac{x}{4(x-1)^2}\ln x\,,\\
C(x) &= \frac{x}{4}\left(\frac{x-6}{2(x-1)}+\frac{3x+2}{2(x-1)^2}\ln x\right),\\
f_1(x,y) &= \frac{x\ln x}{x-1}-\frac{y\ln y}{y-1}\,,\\
f_2(x,y) &= \frac{x\ln y}{(z-x)(x-1)}+\frac{\ln z}{(z-1)(x-1)}\,,\\
f_3(y) &= \frac{1-y+y\ln y}{(y-1)^2}\,,
\end{aligned}
\tag{15}
$$

It should be noted that the coefficient $\tilde{C}_9^{\rm eff}(\mu)$ can be written by three parts:

$$
\tilde{C}_9^{\rm eff}(\mu)=\tilde{C}_9(\mu)+Y_{SD}(\hat{m}_c,\hat{s})+Y_{LD}(\hat{m}_c,\hat{s})\,,
\tag{16}
$$

where the parameters $\hat{m}_c$ and $\hat{s}$ are defined as $\hat{m}_c=m_c/m_b$, $\hat{s}=q^2/m_b^2$. $Y_{SD}(\hat{m}_c,\hat{s})$ describes the short-distance contributions from four-quark operators which can be calculated in the perturbative theory. The function $Y_{SD}(\hat{m}_c,\hat{s})$ is given by:

$$
\begin{aligned}
Y_{SD} &= g(\hat{m}_c,\hat{s})(3C_1+C_2+3C_3+C_4+3C_5+C_6)\\
&- \frac{1}{2}g(1,\hat{s})(4C_3+4C_4+3C_5+C_6)\\
&- \frac{1}{2}g(0,\hat{s})(C_3+3C_4)+\frac{2}{9}(3C_3+C_4+3C_5+C_6),
\end{aligned}
\tag{17}
$$

where the explicit expressions for the g functions can be found in [33]. The long-distance contributions $Y_{LD}(\hat{m}_c,\hat{s})$ originate from the real $c\bar{c}$ intermediate states, i.e., J/ψ, $\psi'\cdots$. The J/ψ family is introduced by the Breit–Wigner distribution for the resonances through the following function[7, 8]:

$$
Y_{\rm LD}=\frac{3\pi}{\alpha^2}C^{(0)}\sum_{V_i=\psi,\psi',\cdots}k_i\,\frac{\Gamma(V_i\to\ell^+\ell^-)m_{V_i}}{m_{V_i}^2-q^2-im_{V_i}\Gamma_{V_i}}\,,
$$

where α is the fine structure constant and $C^{(0)}=(3C_1+C_2+3C_3+C_4+3C_5+C_6)$. The phenomenological parameters k_i for the $\overline{B}\to\overline{K}_0^*(1430)\ell^+\ell^-$ decay can be fixed from $Br(\overline{B}\to J/\psi\overline{K}_0^*(1430)\to\overline{K}_0^*(1430)\ell^+\ell^-)=Br(\overline{B}\to J/\psi\overline{K}_0^*(1430))Br(J/\psi\to\ell^+\ell^-)$. However, since the branching ratio of $\overline{B}\to J/\psi\overline{K}_0^*(1430)$ decay has not been measured yet, we assume that the values of k_i are in the order of one. Therefore, we use $k_1=k_2=1$ in the following numerical calculations[8].

B. Form factors for $\overline{B}\to\overline{K}_0^*(1430)\ell^+\ell^-$ transition

The exclusive $\overline{B}\to\overline{K}_0^*(1430)\ell^+\ell^-$ decay is described in terms of the matrix elements of the quark operators in eq. (9) over meson states, which can be parameterized in terms of the form factors. The needed matrix elements for the calculation of $\overline{B}\to\overline{K}_0^*(1430)\ell^+\ell^-$ decay are:

$$
\left\langle\overline{K}_0^*(1430)(p_{K_0^*})\left|\bar{s}\gamma_\mu(1\pm\gamma_5)b\right|\overline{B}(p_B)\right\rangle = \pm\left[f_+(q^2)(p_B+p_{K_0^*})_\mu+f_-(q^2)q_\mu\right],
\tag{18}
$$

$$
\left\langle\overline{K}_0^*(1430)(p_{K_0^*})\left|\bar{s}i\sigma_{\mu\nu}q^\nu(1\pm\gamma_5)b\right|\overline{B}(p_B)\right\rangle = \frac{\pm f_T(q^2)}{m_B+m_{K_0^*}}\left[(p_B+p_{K_0^*})_\mu q^2-(m_B^2-m_{K_0^*}^2)q_\mu\right],
\tag{19}
$$

$$
\begin{aligned}
\left\langle\overline{K}_0^*(1430)(p_{K_0^*})\left|\bar{s}(1\pm\gamma_5)b\right|\overline{B}(p_B)\right\rangle &= \pm\left\langle\overline{K}_0^*(1430)(p_{K_0^*})\left|\bar{s}\gamma_5 b\right|\overline{B}(p_B)\right\rangle=\mp\frac{1}{m_b+m_s}[f_+(q^2)(p_B+p_{K_0^*}).q+f_-(q^2)q^2] \qquad (20)\\
&= \mp\frac{f_0(q^2)}{m_b+m_s}(m_B^2-m_{K_0^*}^2),\\
\left\langle\overline{K}_0^*(1430)(p_{K_0^*})\left|\bar{s}b\right|\overline{B}(p_B)\right\rangle &= 0\,. \qquad (21)
\end{aligned}
$$

TABLE I: Form factors for $\overline{B}\to\overline{K}_0^*(1430)$ transition obtained within three-point QCD sum rules are fitted to the 3-parameter form.

F	$F(0)$	a_F	b_F
$f_+^{\overline{B}\to\overline{K}_0^*}$	0.31 ± 0.08	0.81	-0.21
$f_-^{\overline{B}\to\overline{K}_0^*}$	-0.31 ± 0.07	0.80	-0.36
$f_T^{\overline{B}\to\overline{K}_0^*}$	-0.26 ± 0.07	0.41	-0.32

where $q=p_B-p_{K_0^*}$ and the function $f_0(q^2)$ has been extracted from

$$f_-(q^2)=\frac{(m_B^2-m_{K_0^*}^2)}{q^2}\left[f_0(q^2)-f_+(q^2)\right]. \tag{22}$$

For the form factors we have used the results of three-point QCD sum rules method [24] in which the q^2 dependence of all form factors is given by

$$F(q^2)=\frac{F(0)}{1-a_F(q^2/m_B^2)+b_F(q^2/m_B^2)^2}, \tag{23}$$

where the values of parameters $F(0)$, a_F and b_F for the $\overline{B}\to\overline{K}_0^*(1430)\ell^+\ell^-$ decay are exhibited in table I.

C. The lepton polarization asymmetries and the CP-violating asymmetry of $\overline{B}\to\overline{K}_0^*(1430)\ell^+\ell^-$

Making use of eq.(9) and the definitions of form factors, the matrix element of the $\overline{B}\to\overline{K}_0^*(1430)\ell^+\ell^-$ decay can be written as follows:

$$\begin{aligned}\mathscr{M} &= \frac{G_F\alpha_{\rm em}}{4\sqrt{2}\pi}V_{ts}^*V_{tb}\,m_B \\ &\left\{[\mathscr{A}(p_B+p_{K_0^*}+\mathscr{B}q)_\mu]\bar{\ell}\gamma^\mu\ell+[\mathscr{C}(p_B+p_{K_0^*}+\mathscr{D}q)_\mu]\bar{\ell}\gamma^\mu\gamma_5\ell+[\mathscr{Q}]\bar{\ell}\ell+[\mathscr{N}]\bar{\ell}\gamma_5\ell\right\},\end{aligned} \tag{24}$$

where the auxiliary functions $\mathscr{A},\cdots,\mathscr{Q}$ are listed in the following:

$$\mathscr{A} = -2\tilde{C}_9^{\rm eff}f_+(q^2)-4(m_b+m_s)C_7^{\rm eff}\frac{f_T(q^2)}{m_B+m_{K_0^*}}, \tag{25}$$

$$\mathscr{B} = -2\tilde{C}_9^{\rm eff}f_-(q^2)+4(m_b+m_s)C_7^{\rm eff}\frac{f_T(q^2)}{(m_B+m_{K_0^*})q^2}(m_B^2-m_{K_0^*}^2), \tag{26}$$

$$\mathscr{C} = -2\tilde{C}_{10}f_+(q^2), \tag{27}$$

$$\mathscr{D} = -2\tilde{C}_{10}f_-(q^2), \tag{28}$$

$$\mathscr{Q} = -2C_{Q_1}f_0(q^2)\frac{(m_B^2-m_{K_0^*}^2)}{m_b+m_s}, \tag{29}$$

$$\mathscr{N} = -2C_{Q_2}f_0(q^2)\frac{(m_B^2-m_{K_0^*}^2)}{m_b+m_s}, \tag{30}$$

with $q=p_B-p_{K_0^*}=p_{\ell^+}+p_{\ell^-}$.

The unpolarized differential decay rate for the $\overline{B}\to\overline{K}_0^*(1430)\ell^+\ell^-$ decay in the rest frame of B meson is given by:

$$\frac{d\Gamma(\overline{B}\to K_0^*\ell^+\ell^-)}{d\hat{s}}=-\frac{G_F^2\alpha_{\rm em}^2m_B}{2^{14}\pi^5}|V_{tb}V_{ts}^*|^2\,v\sqrt{\lambda}\Delta, \tag{31}$$

with

$$\begin{aligned}\Delta &= 16m_\ell m_B^2(1-\hat{r}_{K_0^*})\mathrm{Re}[\mathscr{C}\mathscr{N}^*]+4\hat{s}m_B^2v^2|\mathscr{Q}|^2+16\hat{s}m_\ell^2m_B^2|\mathscr{D}|^2+32m_\ell^2m_B^2(1-\hat{r}_{K_0^*})\mathrm{Re}[\mathscr{C}\mathscr{D}^*] \\ &+ 16\hat{s}m_\ell m_B^2\mathrm{Re}[\mathscr{D}\mathscr{N}^*]+2\hat{s}m_B^2|\mathscr{N}|^2+\frac{4}{3}m_B^4\lambda(3-v^2)|\mathscr{A}|^2 \\ &+ \frac{4}{3}m_B^4|\mathscr{C}|^2\{2\lambda-(1-v^2)(2\lambda-3(1-\hat{r}_{K_0^*})^2)\},\end{aligned} \tag{32}$$

where $v=\sqrt{1-4m_\ell^2/q^2}$, $\hat{s}=q^2/m_B^2$, $\hat{r}_{K_0^*}=m_{K_0^*}^2/m_B^2$ and $\lambda=1+\hat{r}_{K_0^*}^2+\hat{s}^2-2\hat{s}-2\hat{r}_{K_0^*}(1+\hat{s})$.

The CP-violating asymmetry of the $\overline{B}\to\overline{K}_0^*(1430\ell^+\ell^-$ decay is defined by:

$$\mathscr{A}_{CP}(\hat{s})=\frac{\dfrac{d\Gamma}{d\hat{s}}-\dfrac{d\overline{\Gamma}}{d\hat{s}}}{\dfrac{d\Gamma}{d\hat{s}}+\dfrac{d\overline{\Gamma}}{d\hat{s}}}\,, \tag{33}$$

where $\frac{d\Gamma}{d\hat{s}}$ is the unpolarized differential decay rate given by eq.(31) and $\frac{d\overline{\Gamma}}{d\hat{s}}$ is the unpolarized differential decay rate for the antiparticle channel. In order to obtain the latter one we should change the parameters $V_{ts}^*V_{tb}$, λ_{tt} and λ_{tt} of the former one into $V_{ts}V_{tb}^*$, λ_{tt}^* and λ_{tt}^*.

Having obtained the CP-violation asymmetry, let us now consider the single lepton polarization asymmetries associated with the polarized leptons. For this purpose, we first define the following orthogonal unit vectors $s_i^{\pm\mu}$ in the rest frame of $\ell^\pm$, where $i=L,N$ or T are the abbreviations of the longitudinal, normal and transversal spin projections, respectively:

$$\begin{aligned}
s_L^{-\mu} &= \left(0,\vec{e}_L^{\,-}\right)=\left(0,\frac{\vec{p}_{\ell^-}}{|\vec{p}_{\ell^-}|}\right)\,,\\
s_N^{-\mu} &= \left(0,\vec{e}_N^{\,-}\right)=\left(0,\frac{\vec{p}_{K_0^*}\times\vec{p}_{\ell^-}}{\left|\vec{p}_{K_0^*}\times\vec{p}_{\ell^-}\right|}\right)\,,\\
s_T^{-\mu} &= \left(0,\vec{e}_T^{\,-}\right)=\left(0,\vec{e}_N^{\,-}\times\vec{e}_L^{\,-}\right)\,,\\
s_L^{+\mu} &= \left(0,\vec{e}_L^{\,+}\right)=\left(0,\frac{\vec{p}_{\ell^+}}{|\vec{p}_{\ell^+}|}\right)\,,\\
s_N^{+\mu} &= \left(0,\vec{e}_N^{\,+}\right)=\left(0,\frac{\vec{p}_{K_0^*}\times\vec{p}_{\ell^+}}{\left|\vec{p}_{K_0^*}\times\vec{p}_{\ell^+}\right|}\right)\,,\\
s_T^{+\mu} &= \left(0,\vec{e}_T^{\,+}\right)=\left(0,\vec{e}_N^{\,+}\times\vec{e}_L^{\,+}\right)\,,
\end{aligned} \tag{34}$$

where $\vec{p}_{\ell^\mp}$ and $\vec{p}_{K_0^*}$ are in the CM frame of $\ell^-\,\ell^+$ system, respectively. Lorentz transformation is used to boost the components of the lepton polarization to the CM frame of the lepton pair as:

$$\begin{aligned}
\left(s_L^{\mp\mu}\right)_{CM} &= \left(\frac{|\vec{p}_{\ell^\mp}|}{m_\ell}\,,\frac{E_\ell\vec{p}_{\ell^\mp}}{m_\ell\,|\vec{p}_{\ell^\mp}|}\right)\,,\\
\left(s_N^{\mp\mu}\right)_{CM} &= \left(s_N^{\mp\mu}\right)_{RF}\,,\\
\left(s_T^{\mp\mu}\right)_{CM} &= \left(s_T^{\mp\mu}\right)_{RF}\,,
\end{aligned} \tag{35}$$

where RF refers to the rest frame of the corresponding lepton as well as $\vec{p}_{\ell^+}=-\vec{p}_{\ell^-}$ and E_ℓ and m_ℓ are the energy and mass of leptons in the CM frame, respectively.

The single lepton polarization asymmetries can be defined as:

$$\mathscr{P}_i^-(\hat{s})=\frac{\left(\dfrac{d\Gamma}{d\hat{s}}(s_i^-,s_i^+)+\dfrac{d\Gamma}{d\hat{s}}(s_i^-,-s_i^+)\right)-\left(\dfrac{d\Gamma}{d\hat{s}}(-s_i^-,s_i^+)+\dfrac{d\Gamma}{d\hat{s}}(-s_i^-,-s_i^+)\right)}{\left(\dfrac{d\Gamma}{d\hat{s}}(s_i^-,s_i^+)+\dfrac{d\Gamma}{d\hat{s}}(s_i^-,-s_i^+)\right)+\left(\dfrac{d\Gamma}{d\hat{s}}(-s_i^-,s_i^+)+\dfrac{d\Gamma}{d\hat{s}}(-s_i^-,-s_i^+)\right)}\,, \tag{36}$$

$$\mathscr{P}_i^+(\hat{s})=\frac{\left(\dfrac{d\Gamma}{d\hat{s}}(s_i^-,s_i^+)+\dfrac{d\Gamma}{d\hat{s}}(-s_i^-,s_i^+)\right)-\left(\dfrac{d\Gamma}{d\hat{s}}(s_i^-,-s_i^+)+\dfrac{d\Gamma}{d\hat{s}}(-s_i^-,-s_i^+)\right)}{\left(\dfrac{d\Gamma}{d\hat{s}}(s_i^-,s_i^+)+\dfrac{d\Gamma}{d\hat{s}}(s_i^-,-s_i^+)\right)+\left(\dfrac{d\Gamma}{d\hat{s}}(-s_i^-,s_i^+)+\dfrac{d\Gamma}{d\hat{s}}(-s_i^-,-s_i^+)\right)}\,, \tag{37}$$

(38)

where $\frac{d\Gamma(\hat{s})}{d\hat{s}}$'s are calculated in the CM frame. Using these definitions for the single lepton polarization asymmetries, the following explicit forms for $\mathscr{P}_i$'s are obtained:

$$\mathscr{P}_L^\mp = \frac{4vm_B^2}{\Delta}\left\{\pm\frac{4}{3}\lambda m_B^2\mathrm{Re}[\mathscr{A}\mathscr{C}^*]-4m_\ell(1-\hat{r}_{K_0^*})\mathrm{Re}[\mathscr{C}\mathscr{Q}^*]-4m_\ell\hat{s}\mathrm{Re}[\mathscr{D}\mathscr{Q}^*]-2\hat{s}\mathrm{Re}[\mathscr{N}\mathscr{Q}^*]\right\}\,, \tag{39}$$

$$\mathscr{P}_N^{\mp} = \frac{2\pi v\sqrt{\lambda\hat{s}}m_B^3}{\Delta}\Big\{+2m_\ell \mathrm{Im}[\mathscr{D}\mathscr{C}^*]+\mathrm{Im}[\mathscr{N}\mathscr{C}^*]\mp\mathrm{Im}[\mathscr{A}\mathscr{Q}^*]\Big\}, \tag{40}$$

$$\mathscr{P}_T^{\mp} = \frac{\pi\sqrt{\lambda\hat{s}}m_B^3}{\Delta}\Big\{\pm 2\mathrm{Re}[\mathscr{A}\mathscr{N}^*]\pm\frac{4m_\ell}{\hat{s}}(1-\hat{r}_{K_0^*})\mathrm{Re}[\mathscr{A}\mathscr{C}^*]\pm 4m_\ell\mathrm{Re}[\mathscr{A}\mathscr{D}^*]+2v^2\mathrm{Re}[\mathscr{C}\mathscr{Q}^*]\Big\}. \tag{41}$$

IV. NUMERICAL ANALYSIS

In this section, we would like to study the asymmetries $\mathscr{A}_{CP}$ and $\mathscr{P}_i^{\pm}$'s and their averages for the exclusive decay $\overline{B}\to\overline{K}_0^*(1430)\ell^+\ell^-$ in SM and model III of 2HDM. The constraints on 2HDM parameters come from the experimental limits of the electric dipole moments of neutron(NEDM), $B^0-\bar{B}^0$ mixing, ρ_0, R_b and $Br(b\to s\gamma)$[30, 32, 37, 38]. A simple ansatz for $\lambda_{tt}\lambda_{bb}$ would be:

$$\lambda_{tt}\lambda_{bb}=|\lambda_{tt}\lambda_{bb}|\,e^{i\theta}. \tag{42}$$

Considering the restrictions of above references on the parameters of model III of 2HDM and taking $\theta=\pi/2$, we use the following three classes of parameters throughout the numerical analysis[32]:

$$\begin{aligned}
\mathrm{CaseA}: &\ |\lambda_{\mathrm{tt}}| = 0.03;\ \ |\lambda_{bb}|=100,\\
\mathrm{CaseB}: &\ |\lambda_{\mathrm{tt}}| = 0.15;\ \ |\lambda_{bb}|=50,\\
\mathrm{CaseC}: &\ |\lambda_{\mathrm{tt}}| = 0.3;\ \ \ |\lambda_{bb}|=30.
\end{aligned} \tag{43}$$

In addition, in this study we have applied four sets of masses of Higgs bosons which are displayed in tableII[32].

TABLE II: List of the values for the masses of the Higgs particles.

	$m_{H^\pm}$	m_{A^0}	m_{h^0}	m_{H^0}
mass set − 1	200Gev	125Gev	125Gev	160Gev
mass set − 2	160Gev	125Gev	125Gev	160Gev
mass set − 3	200Gev	125Gev	125Gev	125Gev
mass set − 4	160Gev	125Gev	125Gev	125Gev

The corresponding averages are defined by the following equation [9]:

$$\langle\mathscr{A}\rangle=\frac{\displaystyle\int_{4\hat{m}_\ell^2}^{(1-\sqrt{\hat{r}_M})^2}\mathscr{A}\frac{d\mathscr{B}}{d\hat{s}}d\hat{s}}{\displaystyle\int_{4\hat{m}_\ell^2}^{(1-\sqrt{\hat{r}_M})^2}\frac{d\mathscr{B}}{d\hat{s}}d\hat{s}}, \tag{44}$$

where the subscript M refers to $\overline{K}_0^*(1430)$ meson and the subscript $\mathscr{A}$ refers to the asymmetries $\mathscr{A}_{CP}$ and $\mathscr{P}_i^{\pm}$'s. The full kinematical interval of the dilepton invariant mass q^2 is $4m_\ell^2\le q^2\le(m_B-m_M)^2$ for which the long distance contributions (the charmonium resonances) can give substantial effects by considering the two low lying resonances J/ψ and ψ', in the interval of $8\ GeV^2\le q^2\le 14\ GeV^2$. In order to decrease the hadronic uncertainties we use the kinematical region of q^2 for muon as [8]:

$$\mathrm{I}\quad 4m_\ell^2\le q^2\le(m_{J\psi}-0.02\ GeV)^2\ ,$$

$$\mathrm{II}\quad (m_{J\psi}+0.02\ GeV)^2\le q^2\le(m_{\psi'}-0.02\ GeV)^2\ ,$$

$$\mathrm{III}\quad (m_{\psi'}+0.02\ GeV)^2\le q^2\le(m_B-m_M)^2\ ,$$

and for tau as:

$$\text{I} \quad 4m_\ell^2 \leq q^2 \leq (m_{\psi'} - 0.02\ GeV)^2\ ,$$

$$\text{II} \quad (m_{\psi'} + 0.02\ GeV)^2 \leq q^2 \leq (m_B - m_M)^2.$$

We continue our analysis regarding the $\mathscr{A}$'s and their averages by plotting a set of figures (1-11) and presentation of a class of tables (III-VI). In these tables the theoretical and experimental uncertainties corresponding to the SM averages have been evaluated. In such a manner the theoretical uncertainties are extracted from the hadronic uncertainties related to the form factors and the experimental uncertainties originate from the mass of quarks and hadrons and Wolfenstein parameters.

- **Analysis of $\mathscr{A}_{CP}$ asymmetry for $\overline{B} \to \overline{K}_0^* \mu^+ \mu^-$ decay**: The relevant plots in figure(1) show that while the SM prediction of this asymmetry is zero, it is quite sensitive to the variation of the parameters λ_{tt} and λ_{bb}. For example, by enhancing the magnitude of $|\lambda_{tt}\lambda_{bb}|$ the deviation from the SM value is increased. Also, this asymmetry is quite sensitive to the variation of mass of $H^\pm$, this happens due to the reduction of mass of $H^\pm$, such that the deviations from the SM value in mass sets 2 and 4 are more than those in mass sets 1 and 3. By combining the above analyses it is understood that the most deviations from the SM prediction occur in the case C of mass sets 2 and 4. Next to $q^2 = m_{\psi'}^2$ in the afore-mentioned case and mass sets, a deviation around +0.05 is possible as compared to the zero expectation of SM. In addition, it is found out through the corresponding tables (III and IV) that the values of averages show ignorable sensitivities to the presence of new Higgs bosons.
- **Analysis of $\mathscr{P}_L^\mp$ asymmetries for $\overline{B} \to \overline{K}_0^* \mu^+ \mu^-$ decay**: As it is obvious from figure (2) the predictions of all of mass sets throughout the domain $4m_\mu^2 \leq q^2 < (m_B - m_{K_0^*})^2$ apart from $q^2 = (m_B - m_{K_0^*})^2$ are the same and highly coincide with the SM prediction. At $q^2 = (m_B - m_{K_0^*})^2$ the deviation from the SM value in the case A of mass set 3 is more than the others which is +1. At such point the SM prediction is zero. Moreover, it is seen from the tables III and IV that the most deviations of $\langle \mathscr{P}_L^- \rangle$ from the calculated SM value happen in the case C of mass sets 2 and 4 which are very small compared to SM prediction (-3.2% SM). Also it is clear from equation (39) while by ignoring the signs of $\mathscr{P}_L^-$ and $\mathscr{P}_L^+$ in SM the magnitudes of them are the same ($\mathscr{P}_L^+ = -\mathscr{P}_L^-$ in SM), those asymmetries do not have any symmetrical relationship with each other in 2HDM. As it is obvious from figure (3) as well as tables III and IV that the predictions of all of mass sets and cases throughout the interval $4m_\mu^2 \leq q^2 \leq (m_B - m_{K_0^*})^2$ coincide with that of SM very much. The most deviations of $\langle \mathscr{P}_L^+ \rangle$ from the calculated SM value happen in the case C of mass sets 2 and 4 which are -3.2% SM. Ignoring $q^2 = (m_B - m_{K_0^*})^2$ and using the mentioned parameter space for 2HDM, it is found out that $\mathscr{P}_L^+ = -\mathscr{P}_L^-$ in both SM and 2HDM.
- **Analysis of $\mathscr{P}_N^\mp$ asymmetries for $\overline{B} \to \overline{K}_0^* \mu^+ \mu^-$ decay**: The relevant plots in figure (4) show that this asymmetry is quite sensitive to the variation of the parameters λ_{tt} and λ_{bb}. For example, by decreasing the magnitude of $|\lambda_{tt}\lambda_{bb}|$ the deviation from the SM value is increased. Also, this asymmetry is quite sensitive to the variation of masses of H^0 and $H^\pm$, this happens due to the reduction of mass of H^0 and the increment of mass of $H^\pm$, such that the deviations from the SM value in mass sets 3 and 4 are more than those in mass sets 1 and 2. By combining the above analyses it is understood that the most deviation from the SM prediction occurs in the case A of mass set 3. Next to $q^2 = (m_B - m_{K_0^*})^2$ in the afore-mentioned case and mass set, a deviation around -0.09 is possible as compared to SM expectation of zero asymmetry. In addition, it is found out through the corresponding tables that the values of averages show ignorable dependencies to the existence of new Higgs bosons. Also it is clear from equation (40) whereas in SM $\mathscr{P}_N^+ = \mathscr{P}_N^- = 0$, in 2HDM $\mathscr{P}_N^+ = -\mathscr{P}_N^-$.
- **Analysis of $\mathscr{P}_T^\mp$ asymmetries for $\overline{B} \to \overline{K}_0^* \mu^+ \mu^-$ decay**: It is found out from figures (5), (6) and (4) that the asymmetries $\mathscr{P}_T^\mp$ and $\mathscr{P}_N^\mp$ show similar sensitivities to the variations of mass sets and cases. For example, in these asymmetries by decreasing the magnitude of $|\lambda_{tt}\lambda_{bb}|$ or the mass of H^0 and increasing the of mass of $H^\pm$ the deviations from the SM predictions increase. According to this the largest deviations from the SM predictions arise in the case A of mass set 3. Next to $q^2 = (m_B - m_{K_0^*})^2$ in the mentioned case and mass set, deviations around +50% SM and -100% SM are possible for $\mathscr{P}_T^-$ and $\mathscr{P}_T^+$, respectively. In addition, it is found out through the corresponding tables that the most deviations of $\langle \mathscr{P}_T^- \rangle$ and $\langle \mathscr{P}_T^+ \rangle$ from the calculated SM values which happen in the case A of mass

set 3 are +24% SM and −22% SM, respectively. Moreover it is clear from equation (41) while in SM $\mathscr{P}_T^- = -\mathscr{P}_T^+$, there not exist any symmetrical relationship among them in 2HDM. Nevertheless, it is evident from the relevant figures and tables that in cases B and C to a large extent $\mathscr{P}_T^+ = -\mathscr{P}_T^-$.

- **Analysis of $\mathscr{A}_{CP}$ asymmetry for $\overline{B} \to \overline{K}_0^* \tau^+ \tau^-$ decay**: The relevant plots in figure (7) show that while the SM prediction of this asymmetry is zero, it is quite sensitive to the variation of the parameters λ_{tt} and λ_{bb}. For example, by enhancing the magnitude of $|\lambda_{tt}\lambda_{bb}|$ the deviation from the SM value is increased. Also, this asymmetry is quite sensitive to the variation of mass of $H^{\pm}$, this happens due to the reduction of mass of $H^{\pm}$ such that the deviations from the SM value in mass sets 2 and 4 are more than those in mass sets 1 and 3. By combining the above analyses it is understood that the most deviations from the SM prediction occur in the case C of mass sets 2 and 4. Next to $q^2 = m_{\psi'}^2$ in the afore-mentioned case and mass sets, deviations around +0.016 are possible as compared to the zero expectation of SM. In addition, it is found out through the corresponding tables (V and VI) that the values of averages show ignorable sensitivities to the presence of new Higgs bosons.

- **Analysis of $\mathscr{P}_L^{\mp}$ asymmetries for $\overline{B} \to \overline{K}_0^* \tau^+ \tau^-$ decay**: The relevant plots in figure (8) show that this asymmetry is quite sensitive to the variation of the parameters λ_{tt} and λ_{bb}. For example, by decreasing the magnitude of $|\lambda_{tt}\lambda_{bb}|$ the deviation from the SM value is increased. Also, this asymmetry is quite sensitive to the variation of masses of H^0 and $H^{\pm}$, this happens due to the decrease of mass of H^0 and the increase of mass of $H^{\pm}$ such that the deviations from the SM value in mass sets 3 and 4 are more than those in mass sets 1 and 2. By gathering the above analyses it is understood that the most deviation from the SM prediction occurs in the case A of mass set 3. Whereas the SM prediction is zero at $q^2 = (m_B - m_{K_0^*})^2$ a deviation around +0.7 is possible at that point. Besides, it is found out through the corresponding tables that a deviation around -4.9 times of that of SM arises in the case A of mass set 3 at most. Also it is clear from equation (39) while by ignoring the signs of $\mathscr{P}_L^-$ and $\mathscr{P}_L^+$ in SM the magnitudes of them are the same ($\mathscr{P}_L^+ = -\mathscr{P}_L^-$ in SM), those asymmetries do not have any symmetrical relationship with each other in 2HDM. Nevertheless, it is evident from the corresponding figures (8) and (9) and tables that in cases B and C to a large extent $\mathscr{P}_L^+ = -\mathscr{P}_L^-$. The maximum deviations of $\mathscr{P}_L^+$ relative to the SM predictions which are observed in the respective diagrams and tables take place in the case A of mass set 3 which are around +0.7 as compared to SM expectation of zero asymmetry at $q^2 = (m_B - m_{K_0^*})^2$ and +6.6 times of the calculated SM prediction for the related averages.

- **Analysis of $\mathscr{P}_N^{\mp}$ asymmetries for $\overline{B} \to \overline{K}_0^* \tau^+ \tau^-$ decay**: It is clear from figures (10) and (8) that the asymmetries $\mathscr{P}_N^-$ and $\mathscr{P}_L^-$ show the same sensitivities to the variations of mass sets and cases. For instance, in these asymmetries by reducing the magnitude of $|\lambda_{tt}\lambda_{bb}|$ or the mass of H^0 and enhancing the of mass of $H^{\pm}$ the deviations from the SM predictions increase. According to this the largest deviation of $\mathscr{P}_N^-$ from the SM prediction arises in the case A of mass set 3. Next to $q^2 = m_{\psi'}^2$ in the mentioned case and mass set, a deviation around -0.04 compared to the zero prediction of SM is possible for $\mathscr{P}_N^-$. In addition, it is obvious through the respective tables that the most deviation of $\langle \mathscr{P}_N^- \rangle$ from the calculated SM value is -0.024 which happens in the case A of mass set 3. Moreover it is clear from equation (40) while in SM $\mathscr{P}_N^+ = \mathscr{P}_N^- = 0$, in 2HDM $\mathscr{P}_N^+ = -\mathscr{P}_N^-$.

- **Analysis of $\mathscr{P}_T^{\mp}$ asymmetries for $\overline{B} \to \overline{K}_0^* \tau^+ \tau^-$ decay**: Since our analyses for the afore-mentioned all mass sets show that $\mathscr{P}_{T\,2HDM}^- = \mathscr{P}_{T\,SM}^-$ in all cases and $\mathscr{P}_{T\,2HDM}^+ = \mathscr{P}_{T\,SM}^+$ in cases B and C we have only presented the plots of mass set 3 for $\mathscr{P}_T^{\mp}$ in figure (11). In this mass set the most deviation from the SM value for $\mathscr{P}_T^+$ arises somehow in the case A of the range $m_{\psi'}^2 < q^2 < (m_B - m_{K_0^*})^2$ a discrepancy about -25%SM is seen. Also it is clear from the corresponding tables that the largest deviation from the calculated SM anticipation for $\langle \mathscr{P}_T^+ \rangle$ is -15%SM which occurs in the mentioned case and mass set. Moreover it is clear from equation (41)that $\mathscr{P}_T^+ = -\mathscr{P}_T^-$ in SM.

Finally, let us see briefly whether the lepton polarization asymmetries are visitable or not. To measure an asymmetry $\langle \mathscr{A} \rangle$ of the decay with branching ratio $\mathscr{B}$ at $n\sigma$ level in experiment, the required number of events (i.e., the number of $B\overline{B}$) is given by the relation

$$N = \frac{n^2}{\mathscr{B} s_1 s_2 \langle \mathscr{A} \rangle^2} \ ,$$

where s_1 and s_2 are the efficiencies of the leptons. The values of the efficiencies of the τ–leptons differ from 50% to 90% for their different decay modes[39] and the error in τ–lepton polarization is nearly $(10-15)\%$ [40]. So, the error in measurements of the τ–lepton asymmetries is estimated to be about $(20-30)\%$, and the error in obtaining the number of events is about 50%.

According to the above expression for N, in order to measure the single lepton polarization asymmetries in the μ and τ channels at 3σ level, the lowest limit of required number of events are given by(the efficiency of τ–lepton is considered 0.5):

- for $\overline{B}\to\overline{K}_0^*(1430)\mu^+\mu^-$ decay

$$N\sim\begin{cases}10^{24} & (\text{for}\,\langle\mathscr{A}_{CP}\rangle)\,,\\ 10^{7} & (\text{for}\,\langle\mathscr{P}_L^-\rangle,\langle\mathscr{P}_L^+\rangle)\,,\\ 10^{8} & (\text{for}\,\langle\mathscr{P}_T^-\rangle,\langle\mathscr{P}_T^+\rangle)\,,\\ 10^{12} & (\text{for}\,\langle\mathscr{P}_N^-\rangle,\langle\mathscr{P}_N^+\rangle)\,,\end{cases}$$

- for $\overline{B}\to\overline{K}_0^*(1430)\tau^+\tau^-$ decay

$$N\sim\begin{cases}10^{27} & (\text{for}\,\langle\mathscr{A}_{CP}\rangle)\,,\\ 10^{10} & (\text{for}\,\langle\mathscr{P}_L^-\rangle,\langle\mathscr{P}_L^+\rangle)\,,\\ 10^{10} & (\text{for}\,\langle\mathscr{P}_T^-\rangle,\langle\mathscr{P}_T^+\rangle)\,,\\ 10^{13} & (\text{for}\,\langle\mathscr{P}_N^-\rangle,\langle\mathscr{P}_N^+\rangle)\,.\end{cases}$$

V. SUMMARY

In short, in this paper by considering the theoretical and experimental uncertainties in the SM, we have presented a full analysis related to the CP violating effects and single lepton polarization asymmetries for $\overline{B}\to\overline{K}_0^*(1430)\ell^+\ell^-$ decay in model III of 2HDM. At the same time we have compared the results of both μ and τ channels to each other. Also, the minimum required number of events for measuring each asymmetry has been obtained and compared with those in LHC experiments, containing ATLAS, CMS and LHCb, ($\sim 10^{12}$ per year) or expected to be produced at the Super-LHC experiments (supposed to be $\sim 10^{13}$ per year). In conclusion, the following results have been obtained:

i) For the μ channel of single lepton polarization asymmetries ($\mathscr{P}_i^{\mp}(q^2) i=L,N,T$) only the results obtained from case A differ from the SM expectations. This fact indicates that these asymmetries are quite sensitive to the reduction of $|\lambda_{tt}\lambda_{bb}|$. Also, the decrease of the mass of H^0 and simultaneously the increase of the mass of $H^{\pm}$ can enhance the deviations from the SM predictions. Based on the above explanations in all single lepton polarization asymmetries the most deviations from the SM values happen in the case A of mass set 3. On the other hand, for the μ channel of CP violating asymmetry ($\mathscr{A}_{CP}(q^2)$) the results obtained from all cases are different from that of the SM somehow the biggest deviation from the SM anticipation occurs in case C. This fact indicates that this asymmetry is quite sensitive to the enhancement of $|\lambda_{tt}\lambda_{bb}|$. Also, while this asymmetry is quite insensitive to the variation of mass of H^0, the deviations from the SM prediction increase by decreasing the mass of $H^{\pm}$. Based on the above explanations in CP violating asymmetry the most deviations from the SM value happen in the case C of mass sets 2 and 4. Paying attention to the minimum required number of events for detecting each asymmetry it is inferred while all single lepton polarization asymmetries are detectable at LHC, CP violating asymmetry is not measurable in neither LHC nor SLHC.

ii) For the τ channel of $\mathscr{P}_T^-(q^2)$ any sensitivity to the 2HDM parameters is not seen and for the τ channel of other single lepton polarization asymmetries ($\mathscr{P}_T^+(q^2),\mathscr{P}_i^{\mp}(q^2) i=L,N$) only the results obtained from case A differ from the SM expectations. This fact indicates that these asymmetries are quite sensitive to the reduction of $|\lambda_{tt}\lambda_{bb}|$. Also, the decrease of the mass of H^0 and simultaneously the increase of the mass of $H^{\pm}$ can enhance the deviations from the SM predictions. Based on the above explanations in all single lepton polarization asymmetries except that $\mathscr{P}_T^-$ the most deviations from the SM values happen in the case A of mass set 3. On the other hand, for the τ channel of CP violating asymmetry ($\mathscr{A}_{CP}(q^2)$) the results obtained from all cases are different from that of the SM somehow the biggest deviation from the SM anticipation occurs in case C. This fact indicates that this asymmetry is quite sensitive to the enhancement of $|\lambda_{tt}\lambda_{bb}|$. Also, while this asymmetry is quite insensitive to the variation of mass of H^0, the deviations from the SM prediction increase by decreasing the mass of $H^{\pm}$.

Paying attention to the minimum required number of events for detecting each asymmetry it is inferred that $\mathscr{P}_L^{\mp}$ and $\mathscr{P}_T^{\mp}$ are detectable at LHC, $\mathscr{P}_N^{\mp}$ is measurable at SLHC and CP violating asymmetry is not detectable in neither LHC nor SLHC.

iii) For μ channel, in $\langle\mathscr{P}_L^{\mp}\rangle$ the results of cases B and C for all mass sets don't lie between the limits of SM prediction. The maximum deviations of these asymmetries from the calculated values of SM happen in the case C of mass sets 2 and 4 which are -3.2% SM. In $\langle\mathscr{P}_N^{\mp}\rangle$ the results of case A for all mass sets don't lie between the limits of calculated SM prediction. The most deviations from the zero predictions of SM happen in the case A of mass set 3 which are ∓ 0.004. In $\langle\mathscr{P}_T^{\mp}\rangle$ the results of case A for mass sets 1, 3 and 4 don't lie between the limits of SM prediction. The most deviations of $\langle\mathscr{P}_T^{-}\rangle$ and $\langle\mathscr{P}_T^{+}\rangle$ from the calculated values of SM happen in the case A of mass set 3 which are $+24\%$ SM and -22% SM, respectively. In $\langle\mathscr{A}_{CP}\rangle$ the results of all cases for all mass sets don't lie between the limits of SM prediction. The most deviations from the zero prediction of SM happen in the case C of mass sets 2 and 4 which are +0.005.

iv) For τ channel, in $\langle\mathscr{P}_L^{\mp}\rangle$ the results of case A for all mass sets don't lie between the limits of SM prediction. The most deviations of $\langle\mathscr{P}_L^{-}\rangle$ and $\langle\mathscr{P}_L^{+}\rangle$ from the obtained values in SM happen in the case A of mass set 3 which are -4.9 times that of SM and $+6.6$ times that of SM, respectively. In $\langle\mathscr{P}_N^{\mp}\rangle$ the results of cases A and B for all mass sets don't lie between the limits of SM prediction. The most deviations from the zero predictions of SM happen in the case A of mass set 3 which are ∓ 0.024. In $\langle\mathscr{P}_T^{\mp}\rangle$, the results of all cases and mass sets lie between the limits of SM predictions although the most deviation of $\langle\mathscr{P}_T^{+}\rangle$ from the calculated value of SM is -15% SM. In $\langle\mathscr{A}_{CP}\rangle$, the results of all cases and mass sets don't lie between the limits of SM prediction. The most deviations from the zero prediction of SM happen in the case C of mass sets 2 and 4 which are +0.004.

v) By comparing the asymmetries of two channels it is understood that firstly the $\langle\mathscr{A}_{CP}\rangle$ and $\langle\mathscr{P}_T^{\mp}\rangle$ of μ channel are more sensitive to the presence of new Higgs bosons than those of τ channel and secondly the $\langle\mathscr{P}_L^{\mp}\rangle$ and $\langle\mathscr{P}_N^{\mp}\rangle$ of τ channel show more dependency to the existence of new Higgs bosons than those of μ channel.

Finally, it is worthwhile mentioning that although the muon polarization is measured for stationary muons, such experiments are very hard to perform in the near future. The tau polarization can be studied by investigating the decay products of tau. The measurement of tau polarization in this respect is easier than the polarization of muon.

VI. ACKNOWLEDGMENT

The authors would like to thank V. Bashiry for his useful discussions. Support of Research Council of Shiraz University is gratefully acknowledged.

TABLE III: The averaged CP violation and single lepton polarization asymmetries for $\overline{B} \to \overline{K}_0^*(1430)\,\mu^+\mu^-$ in SM and 2HDM for the mass sets 1 and 2 of Higgs bosons and the three cases A ($\theta = \pi/2$, $|\lambda_{tt}| = 0.03$ and $|\lambda_{bb}| = 100$), B ($\theta = \pi/2$, $|\lambda_{tt}| = 0.15$ and $|\lambda_{bb}| = 50$) and C ($\theta = \pi/2$, $|\lambda_{tt}| = 0.3$ and $|\lambda_{bb}| = 30$). The errors shown for each asymmetry are due to the theoretical and experimental uncertainties. The first ones are related to the theoretical uncertainties and the second ones are due to experimental uncertainties. The theoretical uncertainties come from the hadronic uncertainties related to the form factors and the experimental uncertainties originate from the mass of quarks and hadrons and Wolfenstein parameters.

	SM	Case A (Set 1)	Case B (Set1)	Case C (Set1)	Case A (Set 2)	Case B (Set 2)	Case C (Set 2)
$\langle \mathscr{A}_{\rm CP} \rangle$	$0.000^{+0.000+0.000}_{-0.000-0.000}$	$+0.001$	$+0.004$	$+0.004$	$+0.002$	$+0.004$	$+0.005$
$\langle \mathscr{P}_{\rm L}^- \rangle$	$-0.952^{+0.002+0.001}_{-0.002-0.001}$	-0.945	-0.934	-0.929	-0.945	-0.928	-0.922
$\langle \mathscr{P}_{\rm T}^- \rangle$	$-0.158^{+0.009+0.002}_{-0.012-0.002}$	-0.179	-0.156	-0.154	-0.170	-0.154	-0.153
$\langle \mathscr{P}_{\rm N}^- \rangle$	$0.000^{+0.000+0.000}_{-0.000-0.000}$	-0.002	-0.000	-0.000	-0.001	-0.000	-0.000
$\langle \mathscr{P}_{\rm L}^+ \rangle$	$+0.952^{+0.002+0.001}_{-0.002-0.001}$	$+0.950$	$+0.934$	$+0.930$	$+0.948$	$+0.929$	$+0.922$
$\langle \mathscr{P}_{\rm T}^+ \rangle$	$+0.158^{+0.009+0.002}_{-0.012-0.002}$	$+0.140$	$+0.154$	$+0.154$	$+0.149$	$+0.154$	$+0.153$
$\langle \mathscr{P}_{\rm N}^+ \rangle$	$0.000^{+0.000+0.000}_{-0.000-0.000}$	$+0.002$	$+0.000$	$+0.000$	$+0.001$	$+0.000$	$+0.000$

TABLE IV: The same as TABLE III but for the mass sets 3 and 4 of Higgs bosons.

	SM	Case A (Set 3)	Case B (Set3)	Case C (Set3)	Case A (Set 4)	Case B (Set 4)	Case C (Set 4)
$\langle \mathscr{A}_{\rm CP} \rangle$	$0.000^{+0.000+0.000}_{-0.000-0.000}$	$+0.001$	$+0.004$	$+0.004$	$+0.002$	$+0.004$	$+0.005$
$\langle \mathscr{P}_{\rm L}^- \rangle$	$-0.952^{+0.002+0.001}_{-0.002-0.001}$	-0.942	-0.934	-0.929	-0.943	-0.928	-0.922
$\langle \mathscr{P}_{\rm T}^- \rangle$	$-0.158^{+0.009+0.002}_{-0.012-0.002}$	-0.196	-0.156	-0.155	-0.183	-0.155	-0.153
$\langle \mathscr{P}_{\rm N}^- \rangle$	$0.000^{+0.000+0.000}_{-0.000-0.000}$	-0.004	-0.000	-0.000	-0.003	-0.000	-0.000
$\langle \mathscr{P}_{\rm L}^+ \rangle$	$+0.952^{+0.002+0.001}_{-0.002-0.001}$	$+0.952$	$+0.935$	$+0.930$	$+0.950$	$+0.929$	$+0.922$
$\langle \mathscr{P}_{\rm T}^+ \rangle$	$+0.158^{+0.009+0.002}_{-0.012-0.002}$	$+0.123$	$+0.154$	$+0.154$	$+0.136$	$+0.153$	$+0.153$
$\langle \mathscr{P}_{\rm N}^+ \rangle$	$0.000^{+0.000+0.000}_{-0.000-0.000}$	$+0.004$	$+0.000$	$+0.000$	$+0.003$	$+0.000$	$+0.000$

[1] ATLAS Collaboration, "Observation of a new particle in the search for the Standard Model Higgs boson with the ATLAS detector at the LHC", Phys. Lett. **B 716**, 1 (2012).

[2] CMS Collaboration, "Observation of a new boson at a mass of 125 GeV with the CMS experiment at the LHC", Phys. Lett. **B 716**, 30 (2012).

[3] CMS Collaboration, "Observation of a new boson with mass near 125 GeV in pp collisions at $\sqrt{7}$ = 7 and 8 TeV", JHEP **06**, 081 (2013).

[4] T. M. Aliev and M. Savci, Phys. Rev. **D 60**, 014005 (1999).

[5] M. Kobayashi and M. Maskawa, Prog. Theor. phys. **49**,652 (1973).

[6] T. P. Cheng and M. Sher, Phys. Rev. **D 35**, 3484 (1987); **D 44**, 1461 (1991).

[7] F. Kruger. and L.M. Sehgal, Phys.Lett. **B 380**, 199 (1996).

[8] V. Bashiry M. Bayar and K. Azizi, Mod. Phys. Lett. **A 26**, 901 (2011).

[9] T. M. Aliev, M. K. Cakmak, A. Ozpineci and M. Savci, Phys.Rev. **D 64**, 055007 (2001).

TABLE V: The same as TABLE III except for $\overline{B} \to \overline{K}_0^*(1430)\tau^+\tau^-$.

	SM	Case A (Set 1)	Case B (Set1)	Case C (Set1)	Case A (Set 2)	Case B (Set 2)	Case C (Set 2)
$\langle \mathscr{A}_{\rm CP} \rangle$	$0.000^{+0.000+0.000}_{-0.000-0.000}$	$+0.001$	$+0.003$	$+0.003$	$+0.001$	$+0.003$	$+0.004$
$\langle \mathscr{P}_{\rm L}^- \rangle$	$-0.066^{+0.030+0.011}_{-0.077-0.013}$	$+0.147$	-0.056	-0.066	$+0.057$	-0.060	-0.063
$\langle \mathscr{P}_{\rm T}^- \rangle$	$-0.628^{+0.123+0.010}_{-0.127-0.017}$	-0.619	-0.619	-0.612	-0.616	-0.617	-0.609
$\langle \mathscr{P}_{\rm N}^- \rangle$	$0.000^{+0.000+0.000}_{-0.000-0.000}$	-0.013	-0.001	-0.000	-0.008	-0.001	-0.000
$\langle \mathscr{P}_{\rm L}^+ \rangle$	$+0.066^{+0.030+0.011}_{-0.077-0.013}$	$+0.266$	$+0.073$	$+0.066$	$+0.176$	$+0.069$	$+0.065$
$\langle \mathscr{P}_{\rm T}^+ \rangle$	$+0.628^{+0.123+0.010}_{-0.127-0.017}$	$+0.579$	$+0.617$	$+0.612$	$+0.593$	$+0.616$	$+0.609$
$\langle \mathscr{P}_{\rm N}^+ \rangle$	$0.000^{+0.000+0.000}_{-0.000-0.000}$	$+0.013$	$+0.001$	$+0.000$	$+0.008$	$+0.001$	$+0.000$

TABLE VI: The same as TABLE V but for the mass sets 3 and 4 of Higgs bosons.

	SM	Case A (Set 3)	Case B (Set3)	Case C (Set3)	Case A (Set 4)	Case B (Set 4)	Case C (Set 4)
$\langle \mathscr{A}_{\rm CP} \rangle$	$0.000^{+0.000+0.000}_{-0.000-0.000}$	$+0.001$	$+0.003$	$+0.003$	$+0.001$	$+0.003$	$+0.004$
$\langle \mathscr{P}_{\rm L}^- \rangle$	$-0.066^{+0.030+0.011}_{-0.077-0.013}$	$+0.322$	-0.049	-0.060	$+0.197$	-0.054	-0.061
$\langle \mathscr{P}_{\rm T}^- \rangle$	$-0.628^{+0.123+0.010}_{-0.127-0.017}$	-0.611	-0.620	-0.613	-0.617	-0.617	-0.609
$\langle \mathscr{P}_{\rm N}^- \rangle$	$0.000^{+0.000+0.000}_{-0.000-0.000}$	-0.024	-0.002	-0.000	-0.017	-0.001	-0.000
$\langle \mathscr{P}_{\rm L}^+ \rangle$	$+0.066^{+0.030+0.011}_{-0.077-0.013}$	$+0.436$	$+0.081$	$+0.068$	$+0.314$	$+0.075$	$+0.067$
$\langle \mathscr{P}_{\rm T}^+ \rangle$	$+0.628^{+0.123+0.010}_{-0.127-0.017}$	$+0.537$	$+0.617$	$+0.612$	$+0.567$	$+0.615$	$+0.609$
$\langle \mathscr{P}_{\rm N}^+ \rangle$	$0.000^{+0.000+0.000}_{-0.000-0.000}$	$+0.024$	$+0.002$	$+0.000$	$+0.017$	$+0.001$	$+0.000$

[10] G. Buchalla, A. J. Buras and M. E. Lautenbacher, Rev. Mod. Phys. **68**, 1125 (1996).

[11] A. Ali, Int. J. Mod. Phys. **A 20**, 5080 (2005).

[12] B. Aubert et. al, BaBaR Collaboration, Phys. Rev. Lett. **93**, 081802 (2004).

[13] M. I. Iwasaki et. al, BELLE Collaboration, Phys. Rev. **D 72**, 092005 (2005).

[14] K. Abe et. al, BELLE Collaboration, Phys. Rev. Lett. **88**, 021801 (2002).

[15] B. Aubert et. al, BaBaR Collaboration, Phys. Rev. Lett. **91**, 221802 (2003).

[16] A. Ishikawa et. al, BELLE Collaboration, Phys. Rev. Lett. **91**, 261601 (2003).

[17] P. Colangelo, F. De Fazio, P. Santorelli and E. Scrimieri, Phys. Rev. **D 53**, 3672 (1996); Errata D 57, 3186 (1998); A. Ali, P. Ball, L. T. Handoko and G. Hiller, Phys. Rev. **D 61**, 074024 (2000); A. Ali, E. Lunghi, C. Greub and G. Hiller, Phys. Rev. **D 66**, 034002 (2002).

[18] T. M. Aliev, H. Koru, A. Ozpineci, M. Savc, Phys. Lett. **B 400**, 194 (1997); T. M. Aliev, A. Ozpineci, M. Savc, Phys. Rev. **D 56**, 4260 (1997); D. Melikhov, N. Nikitin and S. Simula, Phys. Rev. **D 57**, 6814 (1998).

[19] G. Burdman, Phys. Rev. **D 52**, 6400 (1995); J. L. Hewett and J. D. Walls, Phys. Rev. **D 55**, 5549 (1997); C. H. Chen and C. Q. Geng, Phys. Rev. **D 63**, 114025 (2001).

[20] S. Rai Choudhury, A. S. Cornell, G. C. Joshi and B. H. J. McKellar, Phys. Rev. **D 74**, 054031 (2006).

[21] H. Y. Cheng, C. K. Chua, and C. W. Huang, Phys. Rev. **D 69**, 074025 (2004).

[22] H. Y. Cheng, C. K. Chua, Phys. Rev. **D 69**, 094007 (2004). [16]

[23] C. H. Chen, C. Q. Geng, C. C. Lih and C. C. Liu, Phys. Rev. **D 75**, 074010 (2007).

[24] T. M. Aliev, K. Azizi, M. Savci, Phys. Rev. **D 76**, 074017 (2007).

[25] K. C. Yang, Phys. Lett. **B 695**, 444 (2011).

[26] B. B. Sirvanli, K. Azizi, Y. Lpekoglu, JHEP **1101**, 069 (2011).

[27] V. Bashiry, M. Bayar, K. Azizi, Mod. Phys. Lett. **A 26**, 901 (2011).

[28] F. Falahati, R. Khosravi, Phys. Rev. **D 83** 015010 (2011).

[29] C. Csaki, Mod. Phys. Lett. **A 11**, 599 (1996).

[30] D. Atwood, L. Reina, and A. Soni, Phys. Rev. **D 55**, 3156 (1997).

[31] S. Glashow and S.Weinberg, Phys. Rev. **D 15**, 1958 (1977).

[32] D. Bowser-Chao, K. Cheung, and W. Y. Keung, Phys. Rev. **D 59**, 115006 (1999).

[33] B. Grinstein, M. J. Savage and M. B. Wise, Nucl. Phys. **B 319**, 271 (1989).

[34] A. J. Buras and M. Munz, Phys. Rev. **D 52**, 186 (1995).

[35] Y. B. Dai, C. S. Huang, and H. W. Huang, Phys. Lett. **B 390**, 257 (1997).

[36] P. Ball, JHEP **9809**, 005 (1998).

[37] C. S. Huang and S. H. Zhu, Phys. Rev. **D 68**, 114020 (2003).

[38] Y. B. Dai, C. S. Huang, J. T. Li and W. J. Li, Phys. Rev. **D 67**, 096007 (2003).

[39] G. Abbiendi et al. (OPAL Collaboration), Phys. Lett. **B 492**, 23 (2000).

[40] A. Rouge, Z. Phys. **C 48**, 75 (1990); in Proceedings of the Workshop on τ Lepton Physics, Orsay, France, 1990.

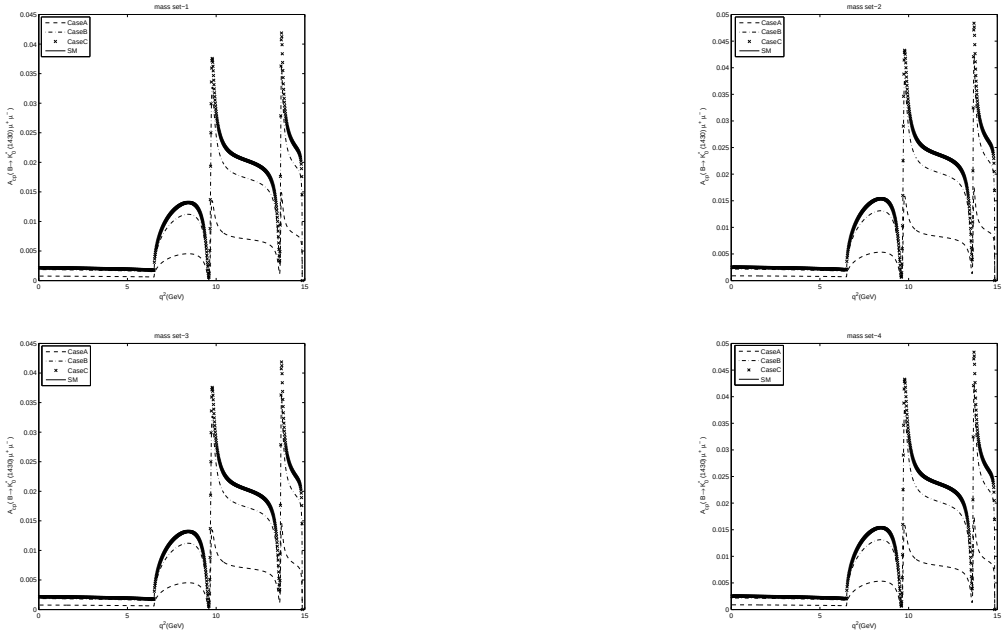

FIG. 1: The dependence of the $\mathscr{A}_{CP}$ polarization on q^2 and the three typical cases of 2HDM, i.e. cases A, B and C and SM for the μ channel of $\overline{B} \to \overline{K}_0^*$ transition for the mass sets 1, 2, 3 and 4.

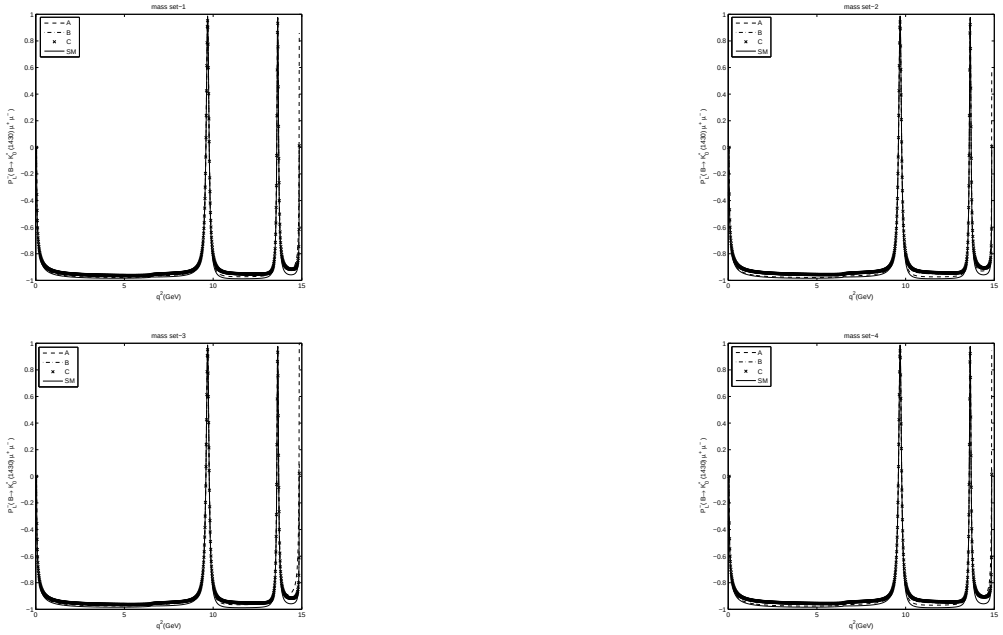

FIG. 2: The dependence of the $\mathscr{P}_L^-$ polarization on q^2 and the three typical cases of 2HDM, i.e. cases A, B and C and SM for the μ channel of $\overline{B} \to \overline{K}_0^*$ transition for the mass sets 1, 2, 3 and 4.

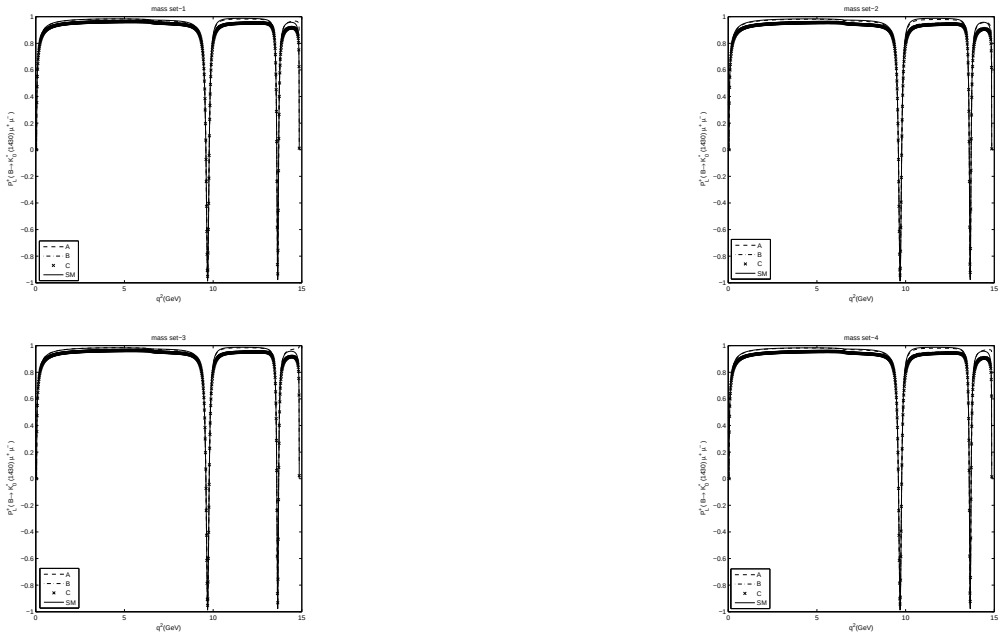

FIG. 3: The dependence of the $\mathscr{P}_L^+$ polarization on q^2 and the three typical cases of 2HDM, i.e. cases A, B and C and SM for the μ channel of $\overline{B} \to \overline{K}_0^*$ transition for the mass sets 1, 2, 3 and 4.

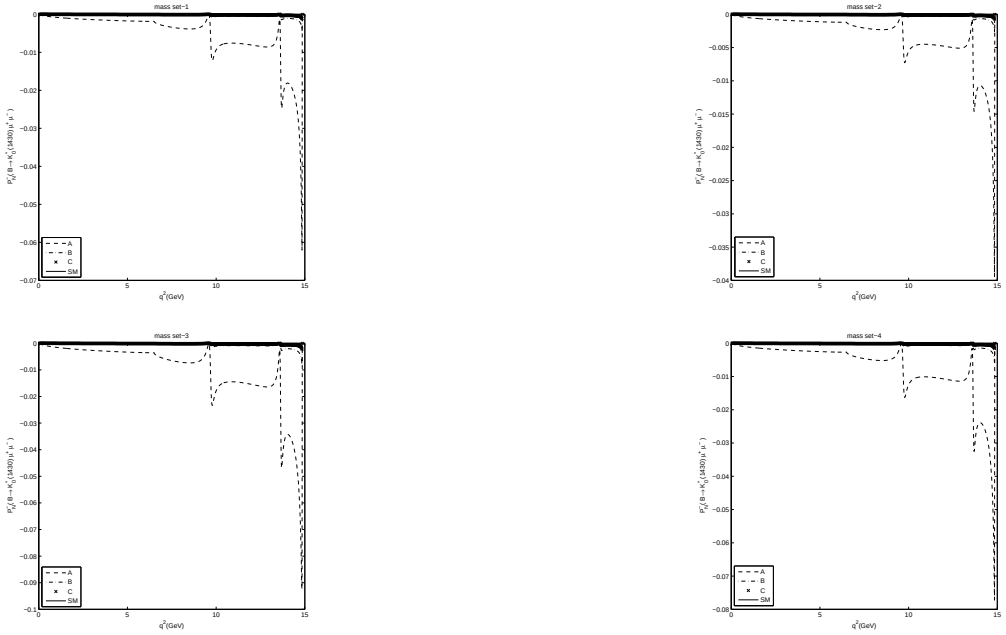

FIG. 4: The dependence of the $\mathscr{P}_N^-$ polarization on q^2 and the three typical cases of 2HDM, i.e. cases A, B and C and SM for the μ channel of $\overline{B} \to \overline{K}_0^*$ transition for the mass sets 1, 2, 3 and 4.

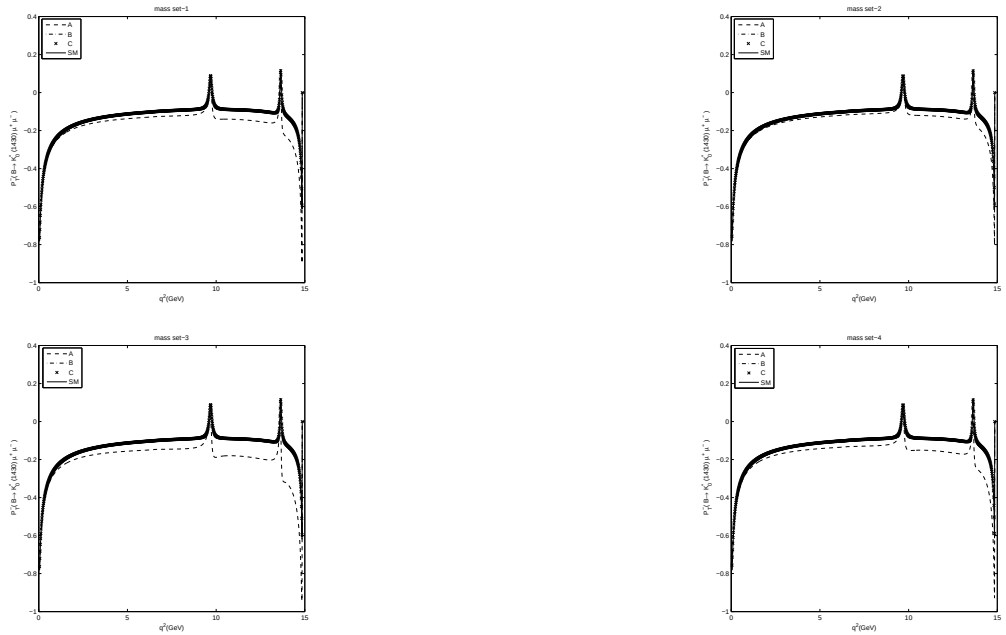

FIG. 5: The dependence of the $\mathscr{P}_T^-$ polarization on q^2 and the three typical cases of 2HDM, i.e. cases A, B and C and SM for the μ channel of $\overline{B} \to \overline{K}_0^*$ transition for the mass sets 1, 2, 3 and 4.

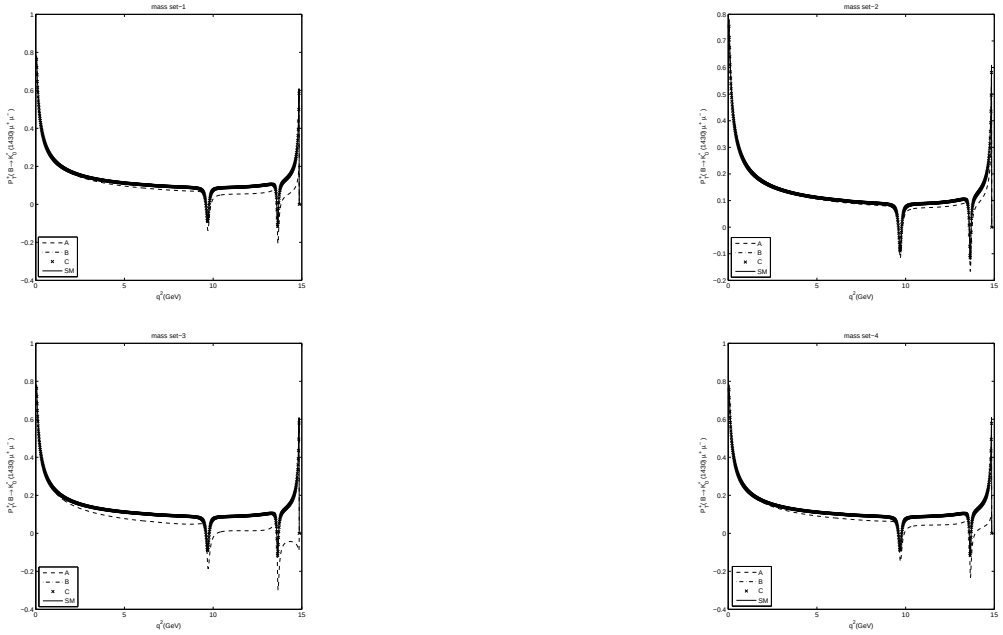

FIG. 6: The dependence of the $\mathscr{P}_T^+$ polarization on q^2 and the three typical cases of 2HDM, i.e. cases A, B and C and SM for the μ channel of $\overline{B} \to \overline{K}_0^*$ transition for the mass sets 1, 2, 3 and 4.

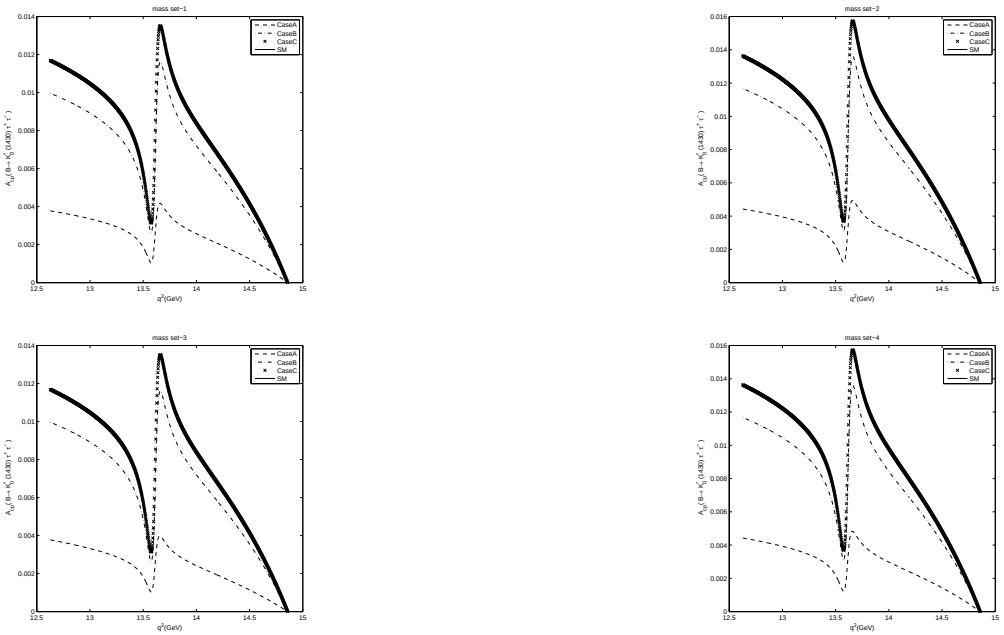

FIG. 7: The dependence of the $\mathscr{A}_{CP}$ polarization on q^2 and the three typical cases of 2HDM, i.e. cases A, B and C and SM for the τ channel of $\overline{B} \to \overline{K}_0^*$ transition for the mass sets 1, 2, 3 and 4.

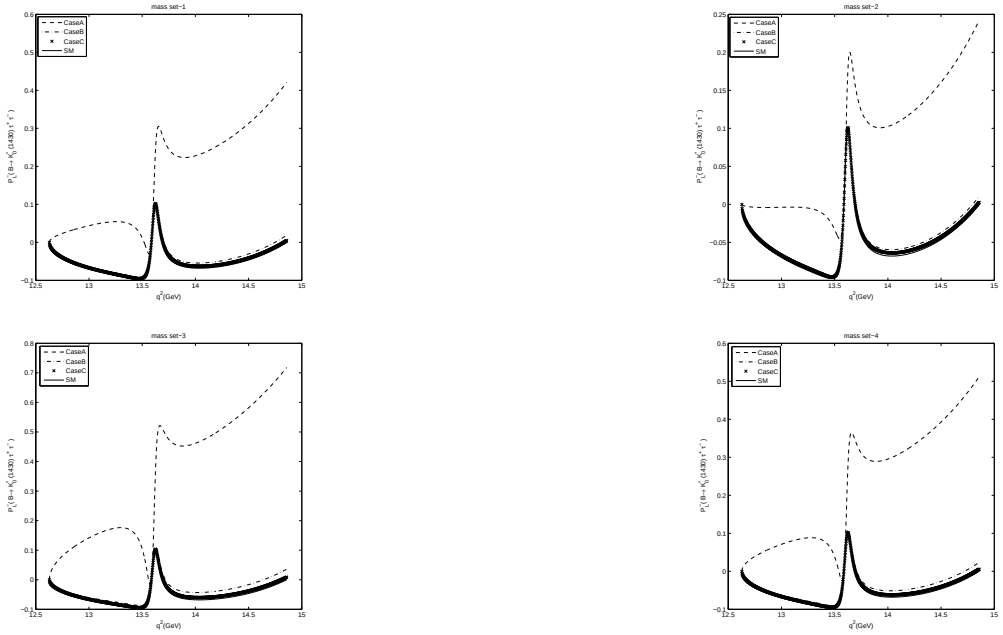

FIG. 8: The dependence of the $\mathscr{P}_L^-$ polarization on q^2 and the three typical cases of 2HDM, i.e. cases A, B and C and SM for the τ channel of $\overline{B} \to \overline{K}_0^*$ transition for the mass sets 1, 2, 3 and 4.

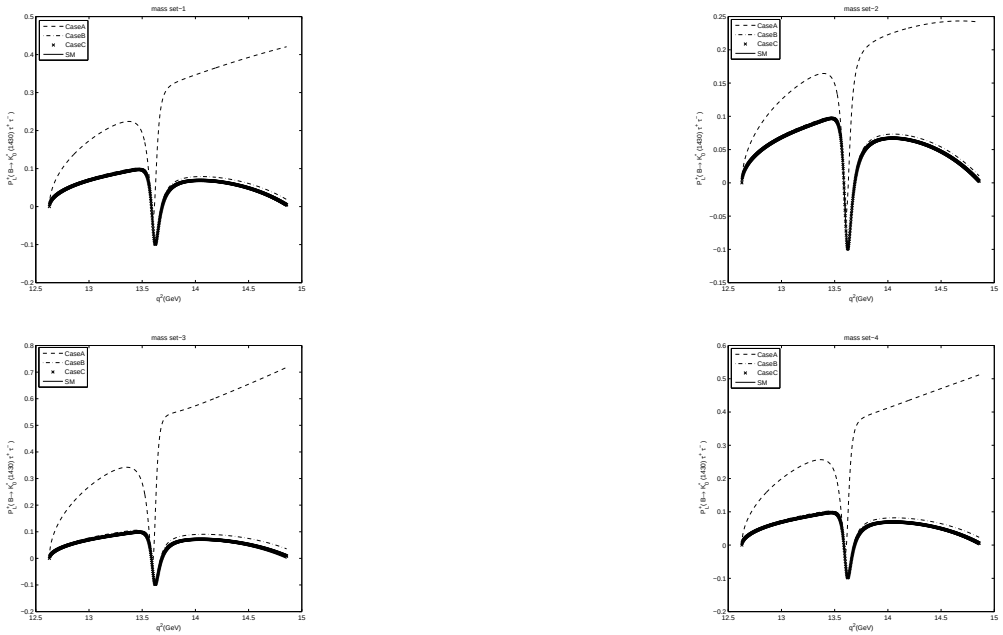

FIG. 9: The dependence of the $\mathscr{P}_L^+$ polarization on q^2 and the three typical cases of 2HDM, i.e. cases A, B and C and SM for the τ channel of $\overline{B} \to \overline{K}_0^*$ transition for the mass sets 1, 2, 3 and 4.

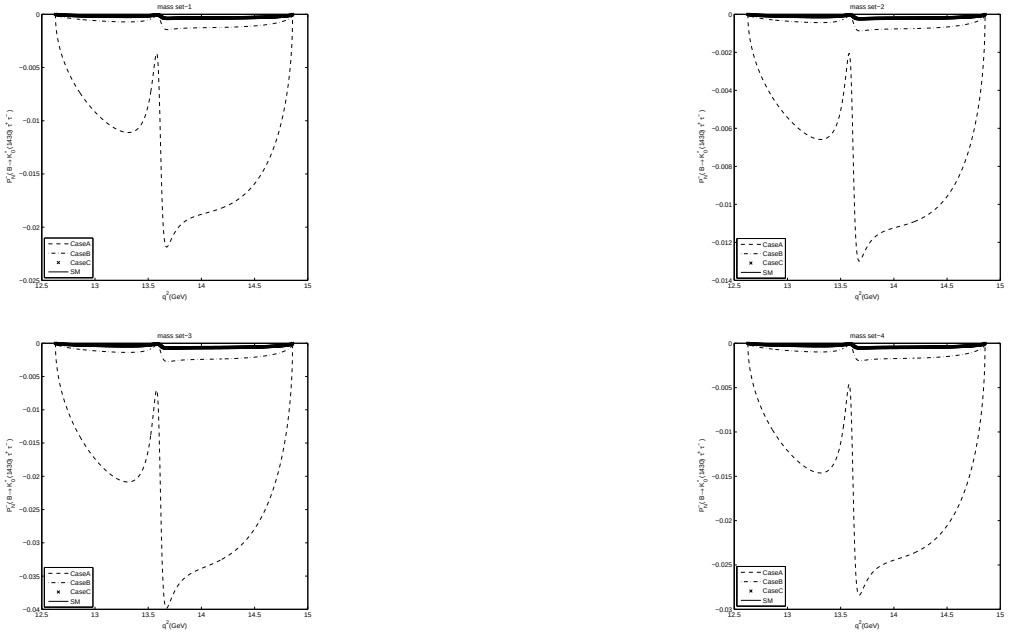

FIG. 10: The dependence of the $\mathscr{P}_N^-$ polarization on q^2 and the three typical cases of 2HDM, i.e. cases A, B and C and SM for the τ channel of $\overline{B} \to \overline{K}_0^*$ transition for the mass sets 1, 2, 3 and 4.

FIG. 11: The dependence of the $\mathscr{P}_T^{\mp}$ polarizations on q^2 and the three typical cases of 2HDM, i.e. cases A, B and C and SM for the τ channel of $\overline{B} \to \overline{K}_0^*$ transition for the mass set 3.